Youngest Toba Tuff deposits in the Gundlakamma river basin, Andhra Pradesh, India and their Role in Evaluating Late Pleistocene Behavioural Change in South Asia

Devara Anil[a], Monika Devi[b,c], James Blinkhorn[d,e], Victoria Smith[f], Satish Sanghode[g], Vrushab Mahesh[a], Zakir Khan[h], P. Ajithprasad[a] and, Naveen Chauhan[b]

[a]Department of Archaeology and Ancient History, Maharaja Sayajirao University of Baroda, Vadodara, India

[b]Luminescence Laboratory, AMOPH Division, Physical Research Laboratory, Ahmedabad, Gujarat, India

[c]Indian Institute of Technology, Gandhinagar, Gujarat, India

[d]Pan-African Evolution Research Group, Max Planck Institute for Geoanthropology, Jena, Germany.

[e]Quaternary Research Centre, Department of Geography, Royal Holloway, University of London, Egham, U.K.

[f]Research Laboratory for Archaeology and the History of Art, School of Archaeology, University of Oxford, Oxford, U.K.

[g]Department of Geology, Savitribhai Phule University, Pune, India.

[h]School of Studies in Ancient Indian History, Culture, and Archaeology, Pt. Ravishankar Shukla University, Raipur, Chhattisgarh, India.

Corresponding Author: Devara Anil (email: devara.anilkumar@gmail.com)

ABSTRACT

The eruption of Toba ca. 75 ka was the largest volcanic eruptive event during the Quaternary, and evidence for this eruption is widespread in terrestrial sediment sequences in South Asia as primary and reworked distal ash deposits. Youngest Toba Tuff horizons (YTT) have been widely employed as isochrons to understand and link regional sediment sequences and the evidence for environmental and cultural change in the archaeological records preserved within them. We identify the YTT deposits at Retlapalle, Andhra Pradesh, India and present the optical ages of the K-feldspar grains recovered from sediments immediately underlying and overlying the tephra horizon. We combine these results with particle size and magnetic susceptibility analyses to establish the depositional conditions of YTT, indicating that accumulation and reworking ceased by ca. 64 ka. We explore the role of YTT deposits as an isochron for examining the impact of the 75 ka Toba super-eruption, highlighting the need for an independent chronological assessment of YTT before using it as a Late Pleistocene chronological marker in reconstructing South Asian palaeo-landscapes and hominin adaptations. Further, our findings support the regional continuity of human occupations within South Asia, spanning the eruption of Toba and the enduring utility of Middle Palaeolithic tools.

Key Words: Youngest Toba Tuff; Late Pleistocene; South Asia; Middle Palaeolithic; Luminescence Dating

INTRODUCTION

The 75 ka eruption of Toba caldera, Indonesia (Mark et al., 2014) is the largest volcanic eruption documented in the past 2 million years. Approximately 2800 km^3 of rhyolitic magma (dense rock equivalent, DRE) was erupted during this event termed the Younger Toba Tuff (YTT) from an enormous vent on the island of Sumatra, resulting in a minimum ashfall of 800 km^3 (Chesner et al., 1991; Costa et al 2014). Distal YTT ash is widespread and found in marine cores from the Indian Ocean and the Arabian Sea (Schulz et al., 1998, 2002; Pattan et al., 1999, 2001, 2002), forms thick terrestrial deposits across South Asia (e.g. Williams and Royce 1982; Acharya and Basu 1993; Jones 2007; Blinkhorn et al. 2014; Singh et al 2022), as well as appearing as cryptotephra in lake cores (e.g. Lane et al., 2013), flowstone records (see Ge and Gao, 2020) and archaeological sites (Smith et al., 2018) thousands of kilometres from the vent. The scale of this eruption has fuelled a debate regarding its impact on the global climate, terrestrial ecosystems, and hominin populations (Rampino and Self, 1993; Ambrose, 1998; Oppenheimer, 2002; Petraglia et al., 2007; Williams et al., 2009). Recent modelling studies have suggested uneven climatic impacts of the eruption, suggesting severe temperature anomalies at higher latitudes contrasting with muted impacts on precipitation at lower latitudes and in the southern hemisphere (Black et al. 2021), which broadly correspond to evidence from fossil and archaeological records for minimal impacts on faunal and human populations (Schulz et al. 2002; Petraglia et al., 2007; Louys, 2012; Clarkson et al., 2020). Nevertheless, the airfall event from the eruption of Toba resulted in a blanket of ca. 4-5 cm of YTT deposited in South Asia (Matthews et al., 2012), with the potential to cause both short- and long-term impacts on the region's geomorphology with significant variability at a landscape scale, which may have ensuing impacts on human populations.

Volcanic ash associated with the YTT was first reported in India in the Son Valley (Williams and Royce, 1982) and ash layers have subsequently been identified across multiple river valleys across peninsular India (Williams and Royce 1982; Acharya and Basu, 1993; Jones 2007; Blinkhorn et al. 2014). Recent studies have employed biotite analyses as the most secure means to resolve between alternate Toba tuffs (Smith et al., 2011). Primary ashfall tephras ca. 4-5 cm thick have been identified in both the Son and Jurreru Valleys, where continuous, uniformly bedded deposits dominated by volcanic glass shards and lacking detrital (non-volcanic) inputs are present (Matthews et al., 2012). More typically, YTT horizons appear as thicker beds up to 5 m thick, indicative of widespread mobilization and concentration of ash across the landscape in topographic low points (e.g., Blinkhorn et al. 2012). In some circumstances, reworked YTT horizons may be disconnected from primary ashfall deposits (Gatti et al., 2011; Neudorf et al., 2014), making their use as an isochron problematic in the absence of geomorphological and chronological control.

Models for the impact of the eruption of Toba on environments and human populations have often relied on YTT to provide a robust isochron (Williams et al 2009). Establishing the depositional and chronological context of YTT deposits is critical for its use as an essential benchmark horizon. This is true regardless of whether it is thought that the eruption of Toba at 75 ka had catastrophic consequences (e.g., Rampino and Self 1992; Ambrose 1998), and immediate changes in environmental and archaeological evidence are anticipated, or whether the impacts of the eruption on human populations have been overstated, without causing any break in cultural transmission or population continuity (e.g., Petraglia et al 2007; Smith et al 2018; Clarkson et al 2020). Notably, these alternatives of a sharp rapid change or continuity and gradual changes in archaeological records before and after the eruption of Toba broadly correspond with competing models for human expansions into South Asia (Blinkhorn and Petraglia, 2017; Groucutt et al., 2015; Mellars et al., 2013; Mishra et al., 2013).

Here we examine the site of Retlapalle, Andhra Pradesh, India (Fig. 1), incorporating evidence from sedimentological, geochemical and geochronological analyses of an excavated sequence. These data are considered with the archaeological evidence to understand hominin behavioural adaptations both at the site and in the broader landscape. This is undertaken to evaluate patterns of behavioural changes spanning the eruption of Toba and illuminate the significance of employing direct geochronological dating on post-Toba deposits to constrain processes of sediment reworking and cultural evolution

THE GUNDLAKAMMA RIVER AND RETLAPALLE STUDY SITE

The Gundlakamma River originates in the Nallamalai Hills ranges, flowing eastward and forming two large lakes at Cumbum and Markapur before altering its course between north-east and south-east before draining into the Bay of Bengal (Fig. 1). The river Gundlakamma has a very narrow flood plain; therefore, the accumulation of Quaternary sediments is also limited. However, three distinct terraces are delineated of which T1 and T2 have a regional presence, whereas the third T3 terrace has developed locally (Reddy and Shah 2004). The basal terrace T1 is flat, narrow and comprises sand and gravel; T2 is made of gravel, sand, silt and volcanic ash. The volcanic ash is observed within the T2 terrace and sandwiched between flood plain sediments. The T3 terrace is mostly carved out of pediment, but in places, it also comprises sand and silt.

Recent Quaternary geological studies identified the presence of volcanic ash concentrated in the upper and middle reaches of the river and attributed it to YTT based on geochemical studies done through the XRF method (Reddy and Shah 2004). Deposits of YTT have also been reported from adjacent river systems, including the Jurreru (Raman and Murty 1997; Petraglia et al., 2007) and the Sagileru (Basu and Biswas 1990; Blinkhorn et al., 2014; Geethanjali et al., 2019). Archaeological surveys of the Gundlakamma valley were first undertaken in the 1950s, indicating the presence of a broad range of Palaeolithic activity

116 within the landscape (Issac 1960). Lower Palaeolithic (Acheulean) and Middle Palaeolithic
117 occurrences are reported as widespread in the Gundlakamma valley, alongside the reported
118 presence of an Upper (Late) Palaeolithic site at Yerragondapalem (Kumari 1987).

119 Recent surveys have identified a further six sites with volcanic ash horizons and 20 new
120 Palaeolithic sites in the upper Gundlakamma valley, including identification of the site of
121 Retlapalle (N15.59°, E79.19°) on the bank of a minor tributary named the Erravagu, which
122 includes both an ash horizon and an artefact bearing horizon (Anil et al. 2020). Where ash
123 beds are present, they appear with a maximum thickness of 50 cm and appear as laterally
124 discontinuous horizons, disrupted by post-depositional erosion (Anil et al., 2020).
125 Preliminary analyses of stone tool assemblages indicate the widespread presence of Middle
126 Palaeolithic technologies that are closely comparable to the Middle Palaeolithic assemblages
127 known from the nearby Jurreru Valley (Anil et al., 2019). To place these archaeological
128 results within a chronostratigraphic framework with a demonstrable relationship to YTT, we
129 conducted excavations at Retlapalle, where survey results indicated the presence of ash
130 deposits and Middle Palaeolithic artefacts.

131 **METHODS**

132 A 1 m wide stepped trench was excavated into a cliff section cut by the Erravagu stream (Fig.
133 4), excavating in 10 cm arbitrary units within discrete sediment units and sieving sediments
134 through 5 mm mesh to control artefact recovery. Sediment samples were recovered at regular
135 intervals throughout the sequence to enable laboratory descriptions. Analysis of the lithic
136 artefacts employed standard terminologies frequently used across South Asia (e.g., Petraglia
137 et al. 2007; Haslam et al. 2012; Blinkhorn et al. 2013; Clarkson et al. 2020).

138 Laser particle size and Loss on Ignition analyses were conducted at Quaternary Research
139 Centre, Department of Geography, Royal Holloway, University of London, Egham, U.K. To

prepare for particle size analysis, sediment samples were first disaggregated in weak hydrochloric acid (0.5 M) to remove post-depositional carbonate cementation, then bathed in 4.4% sodium hexametaphosphate solution for 24 hours to disperse fine particles, agitated in an ultrasonic bath prior to rinsing in purified water and analysis in a Malvern Mastersizer 3000. Results were summarised in Supplementary Table 1. For loss on ignition studies, sediment samples (~10 g) were weighed (to three decimal places, i.e., 0.001g) and heated in a muffle furnace to 105°C, 400°C, 480°C, and 950°C (allowing the sediments to cool to 105°C for weighing between steps) to calculate the proportions of water, carbohydrate, total organic matter, carbonates, and mineral residue. Results are summarised in Supplementary Table 2.

The mineral magnetic analyses were conducted in the Magnetic Laboratory, Department of Geology, Savitribai Phule University, Pune, India. The samples were homogenized using agate mortar and pestle. An average of 9 g of samples was tightly packed into pre-weighted 8 cm^3 cylindrical non-magnetic plastic bottles for magnetic measurements. The weight of the samples was used to calculate the magnetic parameters on a mass-specific basis. Magnetic Susceptibility was measured using Bartington Magnetic Susceptibility Meter with Dual Frequency Sensor. The sensor was calibrated using the standard given by the manufacturer. The measurements were carried out in the 0.1 range with the S.I. unit of $10^{-8}m^3Kg^{-1}$. Magnetic Susceptibility was measured at low frequency at 0.4 kHz (Xlf) and high frequency at 4 kHz (Xhf). The frequency-dependent Susceptibility (Xfd) was calculated from Xlf and Xhf values. Anhysteretic Remanent Magnetisation (ARM) was grown in the samples in a frequency alternating field of 100 mT, while the samples were subjected to a steady field of 0.05 mT. The calibration sample provided by the manufacturer was used to calibrate the magnetometer. An A.F. demagnetizer and an ARM attachment (both of Molspin make) were used. The ARM grew after demagnetizing was measured using a Molspin spinner magnetometer. The Susceptibility of ARM was converted into a mass-specific ARM

(XARM) by dividing it by mass. Natural Remanent Magnetization (NRM) was measured using the Molspin impulse magnetizer by calibrating with the sample provided by the manufacturer. Isothermal Remanent Magnetization (IRM) was grown in steps at different field strengths (25, 50, 100, 200, 300, 400, 500, 700, 800, 1000 for forward and -10, -20, -30, -40, -50, -70, -100, -300 for backfield) using a Molspin impulse magnetizer. The isothermal remanence grew in a 1 T field considered to represent Saturation Isothermal remanent magnetization (SIRM). All remanence measurements were made using the Molspin Impulse magnetizer. Parametric ratios like SOFTIRM, HARDIRM**,** B(0) C.R.**,** S-RATIO-100, S-RATIO300, SIRM/XLF, XARM/XLF, NRM/XLF, XARM/Xfd% were calculated to determine the mineralogy and grain size of the magnetic minerals. Rock magnetic parameters and inter parametric ratios for sediment samples from Retlapalle step trench were summarized in Supplementary Table 3.

Ash samples were collected and analysed at the Research Laboratory for Archaeology and the History of Art, University of Oxford. Glass and biotite crystals from the tephra layers were characterized using the same methods as those used in Blinkhorn et al. (2014).

Sediment samples were analysed for luminescence ages in Physical Research Laboratory, Ahmedabad, India using the procedures discussed in Anil et al. (2022). We measured 20 aliquots per sample using multigrain pIRIRSL on single grain disc. Preheat test was conducted on the natural sample, and an arithmetic mean of 3 aliquots for each preheat was used. The doses for 260º C, 290º C, and 320º C fell within 5% of the estimated palaeo-dose and 320º C was used as pre-heat temparature. The overdispersion (O.D.) in estimated D_e values was relatively low (~8%), as shown in (Fig. 2c & 3c), indicating well bleaching of sediment before burial. Thus, for D_e estimation central age model (CAM) was used. Typical feldspar shine-down growth curves are shown in Fig 2a,b and Fig 3a,b for the Layer B and D samples, respectively. A residual dose of 10.2±0.5 Gy, which is the value of the dose remaining in the sample after five hour extended solar lamp bleaching, was subtracted. The dose reproducibility of the used pIR-IRSL-SAR protocol was tested using the dose recovery test (ratio of recovered to given dose <10% of unity). For the dose recovery test, a known

dose of 237 ± 2 Gy was given in the reader after the solar lamp beaching. The given dose was immediately recovered as an unknown dose. The recovered doses were further corrected for residual doses. The observed dose recovery ratio was 1.09±0.06, indicating that the used pIR-IRSL-SAR protocol has good dose reproducibility. The fading rate measurements were done using the prescription of Auclair et al. (2003) and Huntley and Lamothe (2001). The estimated *g* - values are either less than 1% or negative with ~100% errors (Fig 2d & 3d), suggesting the pIR-IRSL signal is not affected by the anomalous fading (Buylaert et al. 2011). Therefore, no fading corrections were applied to the samples to correct the ages. The concentration of Uranium (U) and Thorium (Th) nuclides were measured using ZnS (Ag) thick source alpha counter and Potassium (K) concentration was measured using NaI (Th) gamma counter. Further, these concentrations were used to estimate the total dose rate assuming infinite matrix assumption, and secular equilibrium for all the nuclides (Table. 1) (Beck and de Planque, 1985). An internal potassium (^{40}K) of 12.5 ± 0.5% (Huntley and Baril, 1997) and 400 ± 100 ppm Rubidium (^{87} Rb) (Huntley and Hancock, 2001) were considered for dose rate estimations.

RESULTS

Stratigraphy and Geoarchaeology

Five discrete sediment units are identified exposed by the Erravagu stream and are directly comparable to the horizons reported by Anil et al., (2020). Layer A comprises reddish sandy silt that was limited in presence in the excavated sequence with a distinct high mineral magnetic signal from underlying deposits but widely evident across the present landscape as a 1.5 m thick deposit (Fig. 4). Layer B is a mid-brown organic-rich (3.6-7%), fine sandy silt with trimodal size distribution and mean particle size ranging from 54 to 130 μm, displaying a gradual decrease in ferromagnetic concentration with depth from surface, and exhibiting a sharp basal contact with Layer C. Layer C comprises, a 42 cm thick reworked volcanic ash horizon, typically characterized as a unimodal very fine sandy coarse silt (mean particle size ranges from 50.2 to 72.8 μm), rich in organic matter (5.9-7.3%), but with low levels of carbonate present (<1.5%). The S-ratio in Layer C depicts a relatively larger domain towards

multi domain (MD) ferrimagnets in agreement with lowering Xfd, XARM, and higher HardIRM, with large fluctuations in mineralogy and ferromagnetic concentration (Fig. 5). A more diffuse contact is observed between Layers C and D. Layer D comprises a reddish-brown trimodal fine sandy medium silt (mean particle size ranges from 52.2 to 70.1 μm), with low levels of carbonates (<2.02%) present, decreased organic components compared to overlying levels (4.7-5.6%) but a comparable and continued gradual decrease in ferromagnetic concentration from Unit B. The basal deposit in the sequence, Layer E, is a pale reddish brown trimodal very fine sandy medium silt, notable for the high proportion of carbonate present (8.9-14%) but with a smaller organic component to overlying levels (3.7-4.3%). A minor peak in ferromagnetic concentration is associated with the upper contact of this unit but otherwise continues a gradual downward decrease. Most of the samples from the Retlapalle section are polymodal silts, suggesting relatively low energy fluvial depositional settings (Fig. 4), which is ideal for the recovery of high integrity archaeological assemblages that are unlikely to have experienced significant artefact mobility. The presence of tephra clearly changes the size distributions as the system is swamped with lots of material of the same size; however, the tephra samples were all fluvially reworked.

Geochemical Fingerprinting

Glass shards from the Retlapalle have 70.77-73.23 wt% SiO_2, 4.15-4.93 wt% K_2O, 2.83-3.46 wt% Na_2O, 0.67-0.90 wt% CaO, and 0.83-1.05 wt% FeO^T (all Fe presented as FeO). These glass compositions shards are similar to tephra shards preserved in the Jurreru Valley, Son Valley, Lenggong, and the YTT proximal samples (Fig. 6a). Biotite occurs as tiny (up to 50 μm) thin sheets of the mica in the Retlapalle distal tephra. The compositional range of biotite crystals in Retlapalle distal tephra is 20.74-23.00 wt% FeO^T, 9.08-9.58 wt% MgO, and 0.23-0.24 wt% F. These are similar to the biotite compositions of the distal YTT units in Malaysia and India (Son Valley, Jurreru Valley; Smith et al., 2011) (Fig. 6b). Raw data for the major

246 elemental compositions of glass and biotite in the samples were provided in Supplementary
247 Table 4. Unlike the glass compositions, the biotite compositions of the YTT are distinct from
248 those samples of the older, large eruptions from Toba (Older Toba Tuff and Middle Toba
249 Tuff). Therefore, the similar composition of the biotite from the Retlapalle tephra (and others
250 in India) to the YTT confirms that the deposit is associated with this last major eruptive event
251 of Toba.

252 **Luminescence Chronology**

253 Sediment samples from layers B and D from the Retlapalle step trench were dated using the
254 post-infrared infrared-stimulated luminescence (p-IR-IRSL) method. The age of layer B
255 above YTT is 64.4±3.9 ka, and the age for the sample from layer D underlying the YTT is
256 76.3± 5.5 ka (Table 1). The overdispersion (OD) in estimated D_e values was quite low (~8%),
257 as shown in Table 1, indicating well bleaching of sediment before burial. Thus, the central
258 age model (CAM) was used for D_e estimation.

259 **Lithic Technology**

260 Our excavations at Retlapalle recovered an assemblage of 102 lithic artefacts from Layer E.
261 All these artefacts were made on coarse to fine grain quartzite. The assemblage consists of
262 one diminutive biface, retouched points and informally retouched flakes (Fig. 7). Due to the
263 small sample size and absence of characteristic artefact types, it is difficult to assign cultural
264 affiliation to these artefacts recovered from the trench. However, systematic surface
265 collections carried out close to the trench that are eroding out from Layer E deposits consists
266 of products of prepared core technology, including Levallois and blade technology, which are
267 most consistent to attributing the assemblage to the Middle Palaeolithic. Although Layer E
268 deposits were not directly dated, a minimum age is provided for these artefacts by the late
269 MIS 5 date from Layer D. A marked increase in the presence of carbonates is observed
270 between Layers D and E, suggesting notable differences in post-depositional conditions

between these units that may be attributable to either decreased precipitation or enhanced seasonality. It is therefore likely that Layer E significantly predates Layer D, and we suggest a late Middle Pleistocene age.

No artefacts were recovered from Layers B or D during our excavations, yet the direct dating of these horizons to 64.4±3.9 ka and 76.3± 5.5 ka respectively provide vital means to interpret patterns of behavioural variability from artefact assemblages deriving from these units found elsewhere in the landscape, which are discussed below.

DISCUSSION

The current study confirms the attribution of volcanic ash deposits in the Gundlakamma basin as YTT through direct geochemical fingerprinting of glass shard and biotite composition. We constrain the deposition and mobility of this tephra within low energy soft sediment contexts to ca. 10 thousand years following the eruption of Toba. Evidence of hominin occupation at the excavated site is restricted to Layer E, which is currently undated but constrained to > 76 ka. However, by constraining the chronology of depositional units that precede and succeed the deposition of YTT across the landscape (Anil et al 2020), we can ascribe archaeological assemblages found elsewhere from Units D and B to timeframes of 76.3± 5.5 ka and 64.4±3.9 ka, respectively. This enables our discussion of the impact of the eruption of Toba and deposition of YTT in the Gundlakamma basin.

The YTT horizon we report is around ten times thicker than primary ashfall deposits identified from marine cores (Schulz et al., 1998, 2002) as well as through direct study of terrestrial sequences (Matthews et al. 2012), clearly indicating the reworking of this ash within the landscape. Our study of mineral magnetics indicates this redeposited tephra as anomalous within the sediment sequence, which otherwise demonstrates considerable continuity, with gradual and consistent changes in ferromagnetic concentrations bracketing

the influx of YTT. Here, the YTT deposits appear as a discrete entity within the basin sediments, become stabilized within the valley in the comparatively short time frame of ~10 ka, and do not appear to have undergone multiple phases of redeposition as may have happened elsewhere (e.g., Son Valley (Neudorf et al 2014); Sagileru Valley (Geethanjali et al 2019)). The rapid stabilization of this depositional landscape following the influx of YTT presents an important context to examine environmental and behavioural changes across the eruption of Toba, which are harder to achieve in contexts where multiple or lengthy episodes of reworking of YTT deposits are evident. More broadly, our study emphasizes the importance of undertaking geomorphological and chronological assessment at a local scale to establish the utility of YTT as a discrete sedimentological and chronological marker and, in this case, to establish the timeframe in which post-Toba landscapes stabilized. Among the available chronometric ages that bracket the final deposition of the YTT deposits in South Asia, the ages reported in current study from Retlapalle are closer to the time of Toba eruption at 75 ka (Table 2). Further research is required at Retlapalle and the Gundlakamma basin to clearly demonstrate the presence of a primary ashfall deposit, which provides the most secure isochron (following Matthews et al. 2012).

The rapid stabilization of low-energy soft sediment deposition observed at Retlapalle following the eruption of Toba is particularly fortuitous for examining its impact on human behavioural change. The identification of Middle Palaeolithic assemblages from Layer E deposits suggests a longstanding inhabitation Gundlakamma basin, which could significantly predate the eruption of Toba and potentially extend into the Middle Pleistocene based on comparable discoveries in Andhra Pradesh which share comparable technologies (Anil et al. 2022). Previous research in the landscape records several sites yielding Middle Palaeolithic artefacts across the upper reaches of the Gundlakamma river basin associated with both Layers B and D (Anil et al. 2020). At Kalagotla, Kagitalagudem and Telladinne lithic

artefacts were identified within deposits directly comparable to Layer D sediments we identified at Retlapalle, directly underlying the YTT horizon, and now attributable to the latter stages of MIS 5, ca. 76.3± 5.5 ka. These stone tool assemblages include the presence of alternate Levallois reduction methods (preferential and recurrent flake; point) alongside discoidal and other radial reduction approaches, as well as a range of expedient reduction strategies. Retouched tools attributed to these late MIS 5 deposits include diverse retouched Levallois flakes and points, diverse scrapers, notches and borers, and the presence of tanged points. The range of technology observed in Layer D deposits, with the combination of alternate Levallois and discoidal reduction schemes and production of a range of retouched toolkits including tanged points that matches closely with evidence from other MIS 5 dated sites across South Asia (Sandhav: Blinkhorn et al. 2019; Katoati: Blinkhorn et al. 2013; Jwalapuram: Clarkson et al 2012; Middle Son Valley: Clarkson et al. 2020; 16R Dune: Blinkhorn 2013; Arjun 3: Corvinus 2002; Bundala: Deraniyagala 1992; Karna; Blinkhorn 2014b; Mehtakheri: Mishra et al. 2013)

At JP Cheruvu and Vemulapeta, within the Gundlakamma river basin, lithic artefacts were recovered in sediments directly comparable to Layer B and overlying YTT deposits (Anil et al. 2020) and now attributable to MIS 4 ca. 64.4±3.9 ka. Reduction strategies evident in these assemblages include preferential Levallois flake and point production, the use of radial reduction practices, as well as more prominent focus on blades evident across cores, blanks and retouched pieces. The prominent presence of Levallois points in the blank assemblages are complemented by the appearance of tanged points amongst the retouched toolkit alongside the appearance of burin production. The presence of Middle Palaeolithic assemblages overlying YTT horizons (Anil et al 2020) is consistent with evidence observed elsewhere in Andhra Pradesh (Jurreru Valley; Clarkson et al. 2012; Sagileru Valley; Blinkhorn et al. 2014a) and across South Asia (Son Valley; Clarkson et al. 2020). The range

of technological variability observed in the Gundlakamma river basin in mid MIS 4 is also comparable to that seen in other Middle Palaeolithic sites across South Asia dating to MIS 4 and 3 (Jwalapuram: Clarkson et al. 2012; Katoati; Blinkhorn et al. 2013; Jetpur; Baskaran et al. 1986; Middle Son Valley: Clarkson et al. 2020; Shergarh TriJunction: Blinkhorn 2014; Bhimbetkha: Bednarik et al. 2005; Orsang: Ajithprasad 2005).

South Asia presents a unique context to examine the impact of the recent eruption of Toba regardless of the potential impacts to regional or global climates, which appear to have had limited influence on broader patterns of cultural evolution (e.g., South African sites (Smith et al 2018)). It is only in South Asia that we have evidence for clear impacts that Toba had on landscapes and hominin populations, manifested in the deposition of a blanket of ash that subsequently swamped drainage networks and patterns of change in behaviour in stone tool assemblages that span this timeframe. In both regional (Jurreru Valley) and more distant (Son Valley) sites, continuity in Middle Palaeolithic technologies preceding and succeeding the eruption of Toba are well documented (Petraglia et al. 2007; Clarkson et al. 2012; 2020). Our findings corroborate this pattern, with substantial continuity observed in lithic technologies derived from Layers D and B in the Gundlakamma basin. Moreover, the comparatively narrow chronological gap between these assemblages further refines evidence for the response of South Asian Middle Palaeolithic hominins to the eruption of Toba, with Layer B assemblages from JP Cheruvu and Vemulapeta now the oldest examples of lithic technology to directly overly YTT horizons, suggesting limited disruption to regional patterns of occupation. Not only does this illustrate the enduring utility of Middle Palaeolithic toolkits to engage with and adapt to substantive environmental challenges occurring at a landscape scale, but also indicates contemporaneity between the deployment of these technologies by South Asian populations and the earliest appearance of *Homo sapiens* in Southeast Asia (e.g., Tam Pa Ling; Demeter et al. 2012) and Australia (Madjebebe; Clarkson et al. 2017;).

CONCLUSION

This study demonstrates a broadly continuous pattern of sedimentation with in the Gundlakamma basin during the Late Pleistocene that has seen limited disruption as a result of the YTT eruption and deposition of tephra across the landscape. Within 10 ky of the eruption reworking of YTT appears to have ceased with the return to a pattern of sedimentation that is comparable those preceding the eruption of Toba re-established by ca. 64 ka. Direct dating of sediment deposits over- and under-lying the YTT horizons enables examination of trajectories of change in hominin behaviour in response to changes within this landscape. This suggests a pattern of continuity that is consistent with wider regional evidence for the persistence in the use of Middle Palaeolithic technologies in South Asia spanning the eruption of Toba.

ACKNOWLEDGEMENTS

The authors acknowledge the Archaeological Survey of India and the Department of Archaeology & Museums, Andhra Pradesh, for granting permission to conduct field surveys in the region. This research is funded by the National Geographic Society Early Career Grant (Grant number #HJ-163ER-17) entitled "Investigating Palaeolithic sites Associated with Youngest Toba Tuff deposits, Southeast India", awarded to Devara Anil. Devara Anil thanks Mr Shashi Mehra, Mr Ravindra Devra, Mr Avinandan Mukherjee, and Mr Ganesh for cooperating during the field surveys. We thank Mr Pullaiah and Mr Venkataiah, residents of Retlapalle village, for their cooperation.

392 **REFERENCES**

393 Acharyya, S. K., and Basu, P. K. 1993. Toba Ash on the Indian Subcontinent and Its
394 Implications for Correlation of Late Pleistocene Alluvium. *Quaternary Research* 40 **(**1**):**
395 10-19.

396 Ajithprasad, P. 2005. Early Middle Palaeolithic: A Transition Phase Between the Upper
397 Acheulian and Middle Palaeolithic Cultures in the Orsang Valley, Gujarat, *Man*
398 *and Environment* 30(2):1-11.

399 Ambrose, S. H. 1998. Late Pleistocene human population bottlenecks, volcanic winter, and
400 differentiation of modern humans. *Journal of Human Evolution* 34 (6)**:** 623-651.

401 Anil, D., P. Ajithprasad, Vrushab Mahesh and Gopesh Jha. 2019. Middle Palaeolthic sites
402 associated with Youngest Toba Tuff deposits from the Middle Gundlakamma Valley,
403 Andhra Pradesh, India. *Heritage: Journal of Multidisciplinary Studies in Archaeology*.
404 Vol. 7, pp:1-14.

405 Anil, D., Ajithprasad, P., Vrushab, M., 2020. Palaeolithic Assemblages associated with
406 Youngest Toba Tuff deposits from the Upper Gundlakamma river basin, Andhra
407 Pradesh, India. In Nupur Tiwari, Vivek Singh and Shashi Mehra (Eds.), *Quaternary*
408 *Geoarchaeology of India. Geol. Soc. London, Spec. Publ.* SP515-2020–187.
409 https://doi.org/10.1144/sp515-2020-187.

410 Anil, Devara., Chauhan, N., Ajithprasad, P., Devi, M., Mahesh, V and Zakir Khan. 2022. An
411 Early presence of Modern Human or Convergent Evolution? A 247 ka Middle
412 Palaeolithic Assemblage from Andhra Pradesh, India. *Journal of Archaeological*
413 *Science: Reports*. 45, 103565. https://doi.org/10.1016/j.jasrep.2022.103565

414 Auclair, M., Lamothe, M., Huot, S., 2003. Measurement of anomalous fading for feldspar
415 IRSL using SAR. *Radiat. Meas.* 37, 487–492.

Bae, C.J., Douka, K., Petraglia, M.D., 2017. On the origin of modern humans: Asian perspectives. Science (80-.). 358. https://doi.org/10.1126/science.aai9067

Baskaran, M., Marathe, A.R., Rajaguru, S.N. & Somayajulu, B.L.K., 1986. Geochronology of Palaeolithic Cultures in the Hiran Valley, Saurashtra, India. *Journal of Archaeological Science* 13, 505-514.

Basu P. K. & Biswas S. (1990) Quaternary ash beds from Eastern India. *Records of the Geological Survey of India* 123: 12.

Beck, H.L., de Planque, G., 1985. Dose rate conversion factors. Health Physics.

Bednarik, R. G., G. Kumar, A. Watchman, and R. G. Roberts. 2005. Preliminary results of the EIP Project. *Rock Art Research* 22:147–197.

Biswas, R.H., Williams, M.A.J., Raj, R., Juyal, N., Singhvi, A.K., 2013. Methodological studies of luminescence dating of volcanic ashes. *Quaternary Geochronology*. 17, 14–25.

Black B.A., Lamarque J.F., Marsh D.R., Schmidt A., Bardeen C.G. 2021. Global climate disruption and regional climate shelters after the Toba supereruption. *Proc Natl Acad Sci U S A.*;118(29):2013046118.

Blinkhorn, J. 2013. A new synthesis of evidence for the Upper Pleistocene occupation of 16R Dune and its southern Asian context. Quaternary International 300:282–291.

Blinkhorn, J., Petraglia, M.D., 2017. Environments and Cultural Change in the Indian Subcontinent: Implications for the Dispersal of Homo sapiens in the Late Pleistocene. *Current Anthropology*. 58, S463–S479. https://doi.org/10.1086/693462.

Blinkhorn, J., Parker, A. G., Ditchfield, P., Haslam, M., & Petraglia, M. 2012. Uncovering a

438 landscape buried by the supereruption of Toba, 74,000 years ago: A multi-proxy
439 environmental reconstruction of landscape heterogeneity in the Jurreru Valley, south
440 India. *Quaternary International*, 258, 135-147.

441 Blinkhorn, J., H. Achyuthan, M. Petraglia, and P. Ditchfield. 2013. Middle Paleolithic
442 occupation in the Thar Desert during the Upper Pleistocene: the signature of a modern
443 human exit out of Africa? *Quaternary Science Reviews* 77:233–238.

444 Blinkhorn, J., Smith, V.C., Achyuthan, H., Shipton, C., Jones, S.C., Ditch, P.D., Petraglia,
445 M.D., 2014a. Discovery of Youngest Toba Tuff localities in the Sagileru Valley,
446 south India, in association with Palaeolithic industries *Quaternary Science*
447 *Review* 105, 239–243. https://doi.org/10.1016/j.quascirev.2014.09.029

448 Blinkhorn, J. 2014b. Late Middle Paleolithic surface sites occurring on dated sediment
449 formations in the Thar Desert. Quaternary International 350:94–104.

450 Blinkhorn, J., P. Ajithprasad, A. Mukherjee, P. Kumar, J.A. Durcan and P. Roberts. 2019.
451 The first directly dated evidence for Palaeolithic occupation on the Indian coast
452 at Sandhav, Kachchh. *Quaternary Science Reviews* 224, 105975.

453 Buylaert, J.-P., Murray, A.S., Thomsen, K.J., Jain, M., 2009. Testing the potential of an
454 elevated temperature IRSL signal from K-feldspar. *Radiat. Meas*. 44, 560–565.

455 Buylaert, J.P., Thiel, C., Murray, A.S., Vandenberghe, D.A.G., Yi, S., Lu, H., 2011. Irsl and
456 post-ir irsl residual doses recorded in modern dust samples from the chinese
457 loess plateau. *Geochronometria* 38, 432–440. https://doi.org/10.2478/s13386-
458 011-0047-0.

459 Chesner, C., Rose, W., Deino, A., Drake, R., Westgate, J.A., 1991. Eruptive history of Earth's

largest Quaternary caldera (Toba, Indonesia) clarified. *Geology* 19, 200–203.

Clarkson, Chris, Jones, Sacha and Harris, Clair (2012). Continuity and change in the lithic industries of the Jurreru Valley, India, before and after the Toba eruption. *Quaternary International*, 258, 165-179. doi: 10.1016/j.quaint.2011.11.007

Clarkson, C., Jacobs, Z., Marwick, B., Fullagar, R., Wallis, L., Smith, M., Roberts, R.G., Hayes, E., Lowe, K., Carah, X., Florin, S.A., McNeil, J., Cox, D., Arnold, L.J., Hua, Q., Huntley, J., Brand, H.E.A., Manne, T., Fairbairn, A., Shulmeister, J., Lyle, L., Salinas, M., Page, M., Connell, K., Park, G., Norman, K., Murphy, T., Pardoe, C., 2017. Human occupation of northern Australia by 65,000 years ago. Nature 547, 306–310. https://doi.org/10.1038/nature22968

Clarkson, C., Harris, C., Li, B., Neudorf, C.M., Roberts, R.G., Lane, C., Norman, K., Pal, J., Jones, S., Shipton, C., Koshy, J., Gupta, M.C., Mishra, D.P., Dubey, A.K., Boivin, N., Petraglia, M., 2020. Human occupation of northern India spans the Toba supereruption ~74,000 years ago. *Nature. Communication. 11*. https://doi.org/10.1038/s41467-020-14668-4.

Corvinus, G. 2002. Arjun 3, a Middle Palaeolithic Site in the Deokhuri Valley, Western Nepal. *Man and Environment* 27 (2), 31–44.

Costa, A., Smith, V. C., Macedonio, G. & Matthews, N. E. The magnitude and impact of the Youngest Toba Tuff super-eruption. Frontiers in Earth Science 2, 59 (2014)

Demeter, F., L. L. Shackelford, A.-M. Bacon, P. Duringer, K. Westaway, T. Sayavongkhamdy, J. Braga, et al. 2012. Anatomically modern human in Southeast Asia (Laos) by 46 ka. Proceedings of the National Academy of Sciences of the USA 109(36):14375–14380

Deraniyagala, S. U. 1992. *The prehistory of Sri Lanka: an ecological perspective*. Colombo: Department of Archaeological Survey, Government of Sri Lanka.

Gatti, E., Durant, A.J., Gibbard, P.L., Oppenheimer, C., 2011. Youngest Toba Tuff in the Son Valley, India : a weak and discontinuous stratigraphic marker. *Quaternary. Science. Rev*iews. 30, 3925–3934. https://doi.org/10.1016/j.quascirev.2011.10.008

Ge, Y., Gao, X., 2020. Understanding the overestimated impact of the Toba volcanic supereruption on global environments and ancient hominins. *Quaternary. International*. 559, 24–33. https://doi.org/10.1016/j.quaint.2020.06.021

Geethanjali, K., Achyuthan, H., Jaiswal, M.K., 2019. The Toba tephra as a late Quaternary stratigraphic marker: Investigations in the Sagileru river basin, Andhra Pradesh, India. *Quaternary International*. 513, 107–123. https://doi.org/10.1016/j.quaint.2019.03.032

Groucutt, H.S., Petraglia, M.D., Bailey, G., Scerri, E.M.L., Parton, A., Clark-Balzan, L., Jennings, R.P., Lewis, L., Blinkhorn, J., Drake, N.A., Breeze, P.S., Inglis, R.H., Devès, M.H., Meredith-Williams, M., Boivin, N., Thomas, M.G., Scally, A., 2015. Rethinking the dispersal of Homo sapiens out of Africa. *Evolutionary Anthropology*. 24. https://doi.org/10.1002/evan.21455

Haslam, M., C. Clarkson, R. G. Roberts, J. Bora, R. Korisettar, P. Ditchfield, A. R. Chivas, et al. 2012. A southern Indian Middle Palaeolithic occupation surface sealed by the 74 Ka Toba eruption: further evidence from Jwalapuram Locality 22. *Quaternary International* 258:148–164.

Huntley, D.J., 2006. An explanation of the power-law decay of luminescence. *J. Phys. Condens. Matter* 18, 1359–1365. https://doi.org/10.1088/0953-8984/18/4/020

505 Huntley, D.J., Baril, M.R., 1997. The K content of the K-feldspars being measured in optical
506 dating or in thermoluminescence dating. Ancint TL 15, 11-13.

507 Huntley, D.J., Hancock, R.G.V., 2001. The Rb contents of the K-feldspar grains being
508 measured in optical dating. Anc. TL 19, 43-46.

509 Huntley, D.J., Lamothe, M., 2001. Ubiquity of anomalous fading in K-feldspars and the
510 measurement and correction for it in optical dating. *Can. J. Earth Sci.* 38, 1093–
511 1106. https://doi.org/10.1139/cjes-38-7-1093

512 Issac, N. 1960. *The Stone age Cultures of Kurnool*. Unpublished PhD. thesis. Pune:
513 University of Poona.

514 Jones, S. C. 2007. The Toba supervolcanic eruption: Tephra-fall deposits in India and
515 Palaeanthropological implications. In: M. D. Petraglia and B. Allchin (Eds.), *The*
516 *Evolution and History of Human Populations in South Asia.* Springer, Berlin, pp. 173-
517 200.

518 Kumari, A. 1987. *Palaeolithic Archaeology of the Gundlakamma basin, Andhra Pradesh.*
519 Unpublished M.Phil. thesis. Guntur: Acharya Nagarjuna University.

520 Lane, C.S., Chorn, B.T., Johnson, T.C., 2013. Ash from the Toba supereruption in Lake
521 Malawi shows no volcanic winter in East Africa at 75 ka. *Proc. Natl. Acad. Sci*. 110,
522 8025–8029. https://doi.org/10.1073/pnas.1301474110

523 Louys, J., 2012. Mammal community structure of Sundanese fossil assemblages from the
524 Late Pleistocene, and a discussion on the ecological effects of the Toba eruption.
525 *Quaternary. International.* 258, 80–87. https://doi.org/10.1016/j.quaint.2011.07.027

526 Mark, D.F., Petraglia, M., Smith, V.C., Morgan, L.E., Barfod, D.N., Ellis, B.S., Pearce, N.J.,
527 Pal, J.N., Korisettar, R., 2014. A high-precision 40Ar/39Ar age for the Young Toba Tuff

528 and dating of ultra-distal tephra: Forcing of Quaternary climate and implications for
529 hominin occupation of India. *Quaternary. Geochronology*. 21, 90–103.
530 https://doi.org/10.1016/j.quageo.2012.12.004.

531

532 Matthews, N., Smith, V., Costa, A., 2012. Ultra-distal tephra deposits from supereruptions:
533 examples from Toba, Indonesia and Taupo Volcanic Zone, New Zealand. *Quaternary*
534 *International*, 258 (0): 54-79. https://doi.org/10.1016/j.quaint.2011.07.010

535 Mellars, P., Gori, K.C., Carr, M., Soares, P. a., Richards, M.B., 2013. Genetic and
536 archaeological perspectives on the initial modern human colonization of southern Asia.
537 *Proc.Natl.Acad.Sci. U.S.A.*110,10699–10704. https://doi.org/10.1073/pnas.1306043110.

538 Mishra, S., Chauhan, N., Singhvi, A.K., 2013. Continuity of Microblade Technology in the
539 Indian Subcontinent Since 45 ka: Implications for the Dispersal of Modern Humans.
540 *PLoS One 8*, e69280. https://doi.org/10.1371/journal.pone.0069280

541 Neudorf, C.M., Roberts, R.G., Jacobs, Z., 2014. Testing a model of alluvial deposition in the
542 Middle Son Valley, Madhya Pradesh, India — IRSL dating of terraced alluvial
543 sediments and implications for archaeological surveys and palaeoclimatic
544 reconstructions. *Quaternary Science. Reviews*. 89, 56–69.
545 https://doi.org/10.1016/j.quascirev.2014.02.004

546 Oppenheimer, C., 2002. Limited global change due to the largest known Quaternary eruption,
547 Toba E74 kyr BP ? *Quaternary Science Reviews* 21, 1593–1609.

548 Pattan, J. N., Shane, P. A. R., Pearce, N. J. G., Banakar, V. K., and Parthiban, G. 2001. An
549 occurrence of ~ 74 ka Youngest Toba tephra from the western continental margine of
550 India. *Current Science* 80 (10)**:** 1322-1326.

551 Pattan, J. N., Shane, P., and Banakar, V. K. 1999. New occurrence of Youngest Toba Tuff in
552 abyssal sediments of the Central Indian Basin. *Marine Geology* 155 (3-4)**:** 243-248.

553 Petraglia, M., Korisettar, R., Boivin, N., Clarkson, C., Ditchfield, P., Jones, S., Koshy, J.,
554 Lahr, M.M., Oppenheimer, C., Pyle, D., Roberts, R., Schwenninger, J.-L., Arnold, L.,
555 White, K., 2007. Middle Paleolithic assemblages from the Indian subcontinent before
556 and after the Toba supereruption. *Science* 317, 114–6.
557 https://doi.org/10.1126/science.1141564

558

559 Petraglia, M. D., P. Ditchfield, S. Jones, R. Korisettar, and J. N. Pal. 2012. The Toba volcanic
560 super-eruption, environmental change, and hominin occupation history in India over the
561 last 140,000 years. *Quaternary International* 258:119–134.

562 Raman P. K. & Murty V. N. (1997) *Geology of Andhra Pradesh*. Geological Society of India,
563 Bangalore.

564 Rampino, M. R., and Self, S. 1992. Volcanic winter and accelerated glaciation following the
565 Toba super-eruption. Nature 359 (6390)**:** 50.

566 Rampino, M. R., and Self, S. 1993. Climate-Volcanism Feedback and the Toba Eruption of
567 ~74,000 Years Ago. *Quaternary Research* 40 (3)**:** 269.

568 Reddy, M.K and B.M. Shah. 2004. Quaternary Geological Studies with Special Emphasis On
569 Volcanic Ash And Neotectonism in Gundlakamma River Basin Of Guntur And
570 Prakasham Districts, Andhra Pradesh. *Unpublished progress report of Geological*
571 *Survey of India 2003-04*.

572 Schulz, H., Emeis, K.-C., Erlenkeuser, H., von Rad, U., Rolf, C., 2002. The Toba volcanic

573 event and interstadial/stadial climates at the marine isotopic stage 5 to 4 transition in the
574 northern Indian Ocean. *Quaternary Research* 57, 22-31.

575 Schulz, H., von Rad, U., and Erlenkeuser, H. 1998. Correlation between Arabian Sea and
576 Greenland climate oscillations of the past 110,000 years. *Nature* 393 (6680)**:** 54-57.

577 Singh, Ajab., Srivastava Ashok K., Chauhan Naveen, 2022. Luminescence Dating and
578 Bracketing Time of the Youngest Toba Tuff Deposits in the Quaternary Sediments of
579 Purna Alluvial Basin, Central India. *Journal of Earth Science*, 33(4): 1007–1016.
580 https://doi. org/10.1007/s12583-020-1357-z. http://en.earth-science.net

581 Smith, E.I., Jacobs, Z., Johnsen, R., Ren, M., Fisher, E.C., Oestmo, S., Wilkins, J., Harris,
582 J.A., Karkanas, P., Fitch, S., Ciravolo, A., Keenan, D., Cleghorn, N., Lane, C.S.,
583 Matthews, T., Marean, C.W., 2018. Humans thrived in South Africa through the Toba
584 eruption about 74,000 years ago. *Nature* 555, 511–515.
585 https://doi.org/10.1038/nature25967

586 Smith, V. C., Pearce, N. J. G., Matthews, N. E., Westgate, J. A., Petraglia, M. D., Haslam,
587 M., Lane, C. S., Korisettar, R., and Pal, J. N. 2011. Geochemical fingerprinting of the
588 widespread Toba tephra using biotite compositions. *Quaternary International* 246 (1-2)**:**
589 97-104.

590 Westgate, J. A., Shane, P. A. R., Pearce, N. J. G., Perkins, W. T., Korisettar, R., Chesner, C.
591 A., Williams, M. A. J., and Acharyya, S. K. 1998. All Toba Tephra Occurrences across
592 Peninsular India Belong to the 75,000 yr B.P. Eruption. *Quaternary Research* 50 (1)**:**
593 107-112.

594 Williams, M. A. J., Ambrose, S. H., van der Kaars, S., Ruehlemann, C., Chattopadhyaya, U.,
595 Pal, J., and Chauhan, P. R. 2009. Environmental impact of the 73 ka Toba supereruption
596 in South Asia. *Palaeogeography, Palaeoclimatology, Palaeoecology* 284 (3-4)**:** 295-

314.

Williams, M., Royce, K., 1982. Quaternary geology of the middle Son valley, north-central India: implications for prehistoric Archaeology. *Palaeogeogr. Palaeoclimatol. Palaeoecol*. 38, 139–162.

List of Tables

List of Figures

633

634 Figure. 6: a: Glass shard compositions (normalized to 100%) from Retlapalle tephra (black
635 diamonds) compared with published proximal YTT data (grey triangles; from Smith et al.,
636 2011). b: Biotite composition of crystals from the deposits at Retlapalle compared with those
637 from the tephra in the Son and Jurerru valleys and proximal samples of OTT, MTT And YTT
638 (data from Smith et al., 2011).

639 Figure. 7: Representative Lithic Artefacts from Layer E at the Retlapalle step trench. a and d:
640 Cores; b, c, f, g, h and j: Flakes; e: Retouched piece; i: Diminutive Handaxe.

641

642

Table. 1: Dose rate data, D_e values and OSL ages for the sediment samples from the step trench at Retlapalle

Sample Code	Depth (cm)	Radionuclide activity[a]				Equivalent doses				OSL age (ka)
		U (ppm)	Th (ppm)	K (%)	Total Dose rate[b,c] (Gy/ka)	No. of aliquots/ grains	Water content (%)	OD (%)	D_e (Gy)[d]	
RTP-18-1	60	2.8±0.3	8.4±1.0	1.5±0.07	3.03±0.17	19	20.6	7.1	193.8±4.5	**64.4±3.9**
RTP-18-2	110	2.6±0.6	11.7±2.2	1.4±0.09	3.07±0.21	20	20.1	8.2	233.7±5.6	**76.3±5.5**

[a] Radioactivity measurement was made on the dried, homogenized and powered sample by gamma-ray spectrometry and alpha counting.

[b] Includes cosmic-ray dose rate

[c] 12.5±0.5% and 200±20 ppm Rubidium (^{87}Rb) concentrations were used to estimate the internal dose rate

[d] after subtracting a residual dose of 10.2 Gy

Table. 2: Sites with Luminescence ages bracketing the YTT deposits in South Asia

Site	Below YTT (ka)	YTT (ka)	Above YTT (ka)	Method	Reference
Jwalapuram 22, Jurreu Valley, Andhra Prdesh	85	-	35	OSL	Haslam et al 2012
Jwalapuram 3, Jurreu Valley, Andhra Prdesh	77±6	-	< 55	OSL	Petraglia et al 2012
Ghoghara, Son Valley, Madhya Pradesh	53±2.6	-	50±2.6	OSL	Neudorf et al 2014
Khunteli, Son Valley, Madhya Pradesh	53±2.1	-	51±3	OSL	Neudorf et al 2014
Khunteli, Son Valley, Madhya Pradesh	61±7	82±13	-	OSL	Biswas et al 2013
Rehi, Son Valley, Madhya Pradesh	83±9 and 70±9	81±15	40±5	OSL	Biswas et al 2013
Tejpur, Madhumati, Gujarat	74±6	71±9	60±7	OSL	Biswas et al 2013
Bori, Kukdi river, Maharasthra	-	27±3	-	OSL	Biswas et al 2013
Morgaon, Karha river, Maharasthra	-	41±5	-	OSL	Biswas et al 2013
Vankamari I, Sagileru river, Andhra Pradesh	64±7	-	48±4	OSL	Geethanjali et al 2019
Vankamari I, Sagileru river, Andhra Pradesh	22±3	-	2.3±0.1	OSL	Geethanjali et al 2019
Sagileru Bridge, Sagileru river, Andhra Pradesh	67±2	-	65±3	OSL	Geethanjali et al 2019
Singampalli, Sagileru, Andhra Pradesh	28±2	-	0.3±0.01	OSL	Geethanjali et al 2019
Ainavolu, Gundlakamma river, Andhra Pradesh	57±5	-	22±3	OSL	Geethanjali et al 2019
Hudki, Purna river, Maharasthra	70±4	-	57±5	OSL	Singh et al 2022
Sukali, Purna river, Maharasthra	66±5	-	67±4	OSL	Singh et al 2022
Retlapalle, Gundlakamm river, Andhra Pradesh	**76.3±5.5**	-	**64.4±3.9**	OSL	Current study

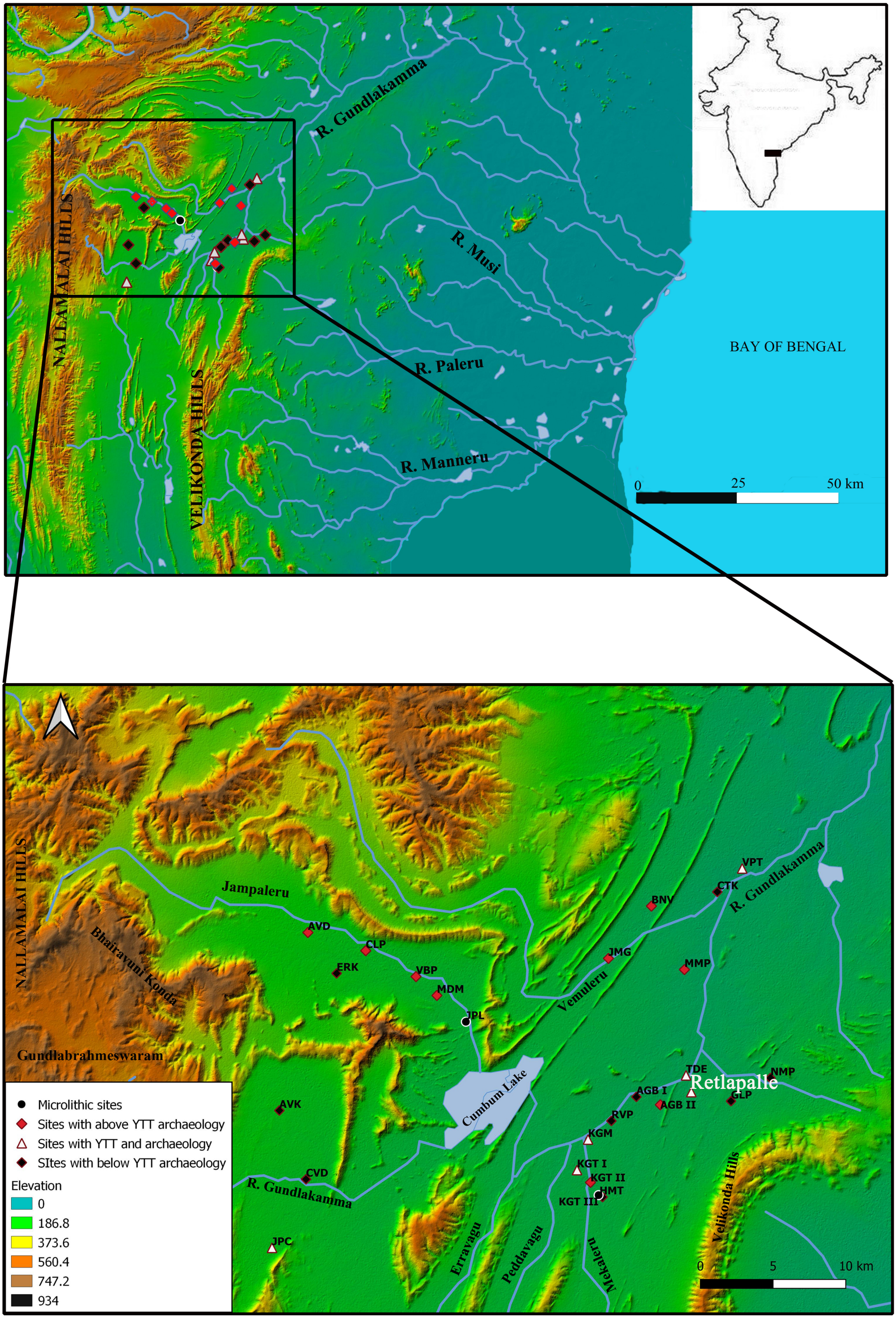
R. Gundlakamma
NALLAMALAI HILLS
R. Musi
R. Paleru
VELIKONDA HILLS
R. Manneru
BAY OF BENGAL
0
25
50 km
NALLAMALAI HILLS
Jampaleru
Bhairavuni Konda
AVD
CLP
ERK
VBP
MDM
JPL
Gundlabrahmeswaram
AVK
CVD
R. Gundlakamma
JPC
Cumbum Lake
Vemuleru
JMG
BNV
VPT
CTK
R. Gundlakamma
MMP
TDE
NMP
Retlapalle
AGB I
AGB II
GLP
RVP
KGM
KGT I
KGT II
HMT
KGT III
Erravagu
Peddavagu
Mekaleru
Velikonda Hills
0
5
10 km
Microlithic sites
Sites with above YTT archaeology
Sites with YTT and archaeology
SItes with below YTT archaeology
Elevation
0
186.8
373.6
560.4
747.2
934

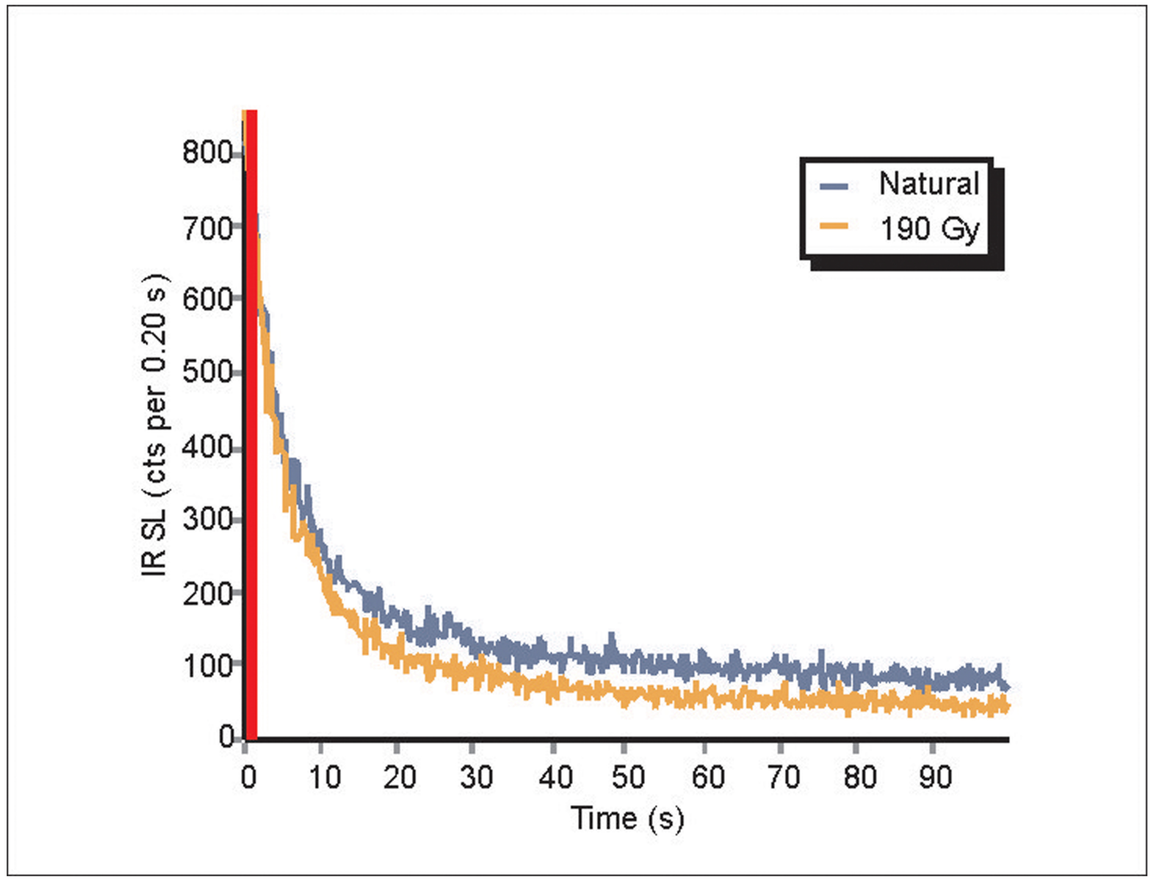
IR SL (cts per 0.20 s)
Time (s)
Natural
190 Gy
0
100
200
300
400
500
600
700
800
0
10
20
30
40
50
60
70
80
90

a

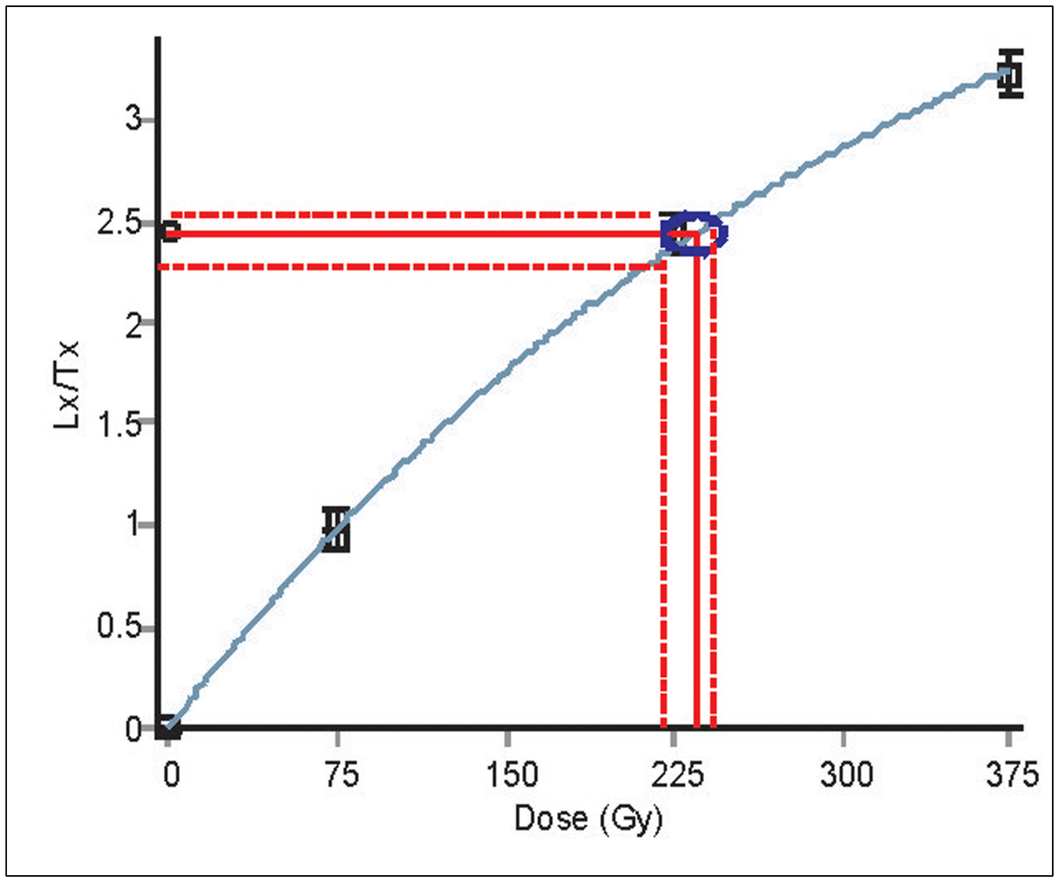
Lx/Tx
Dose (Gy)
0
0.5
1
1.5
2
2.5
3
0
75
150
225
300
375

b

RTP-18-1

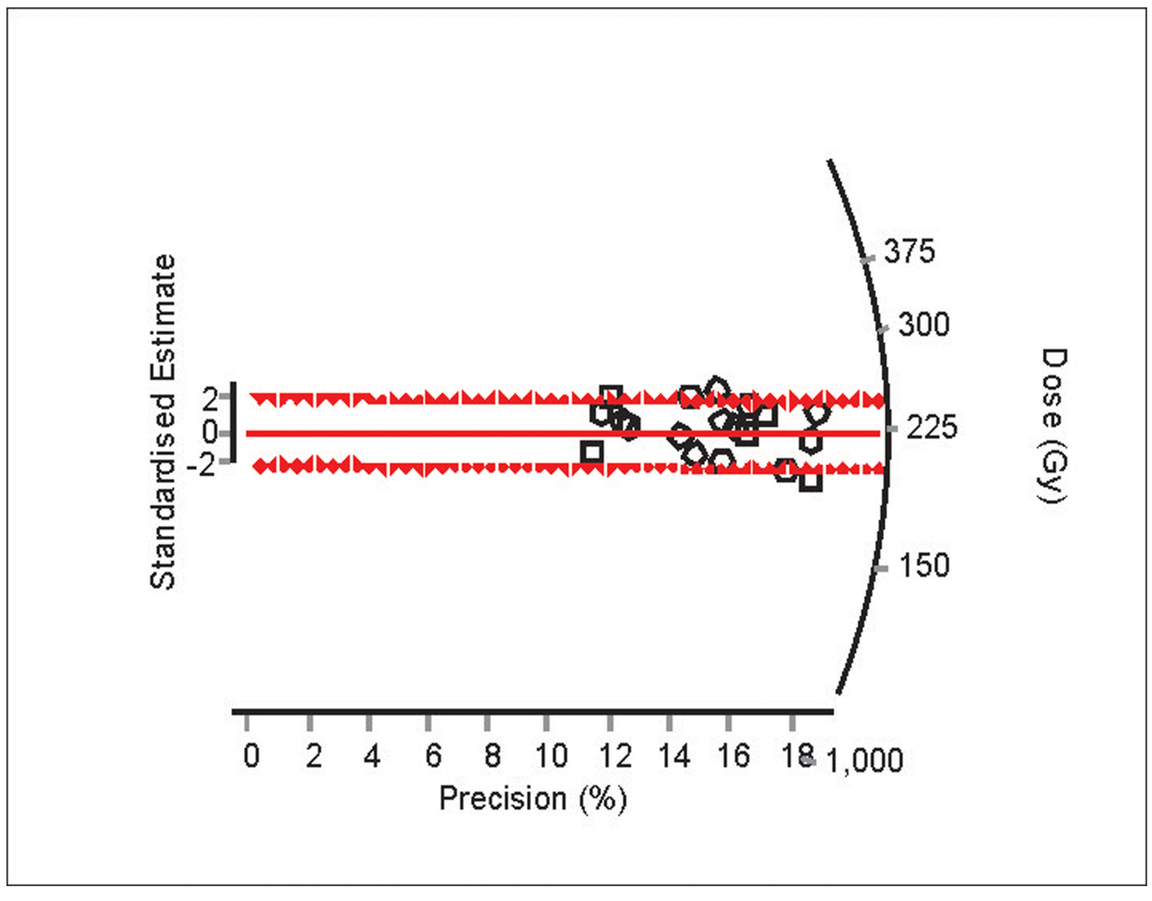
Standardised Estimate
Precision (%)
Dose (Gy)
2
0
-2
0
2
4
6
8
10
12
14
16
18
375
300
225
150
1,000

c

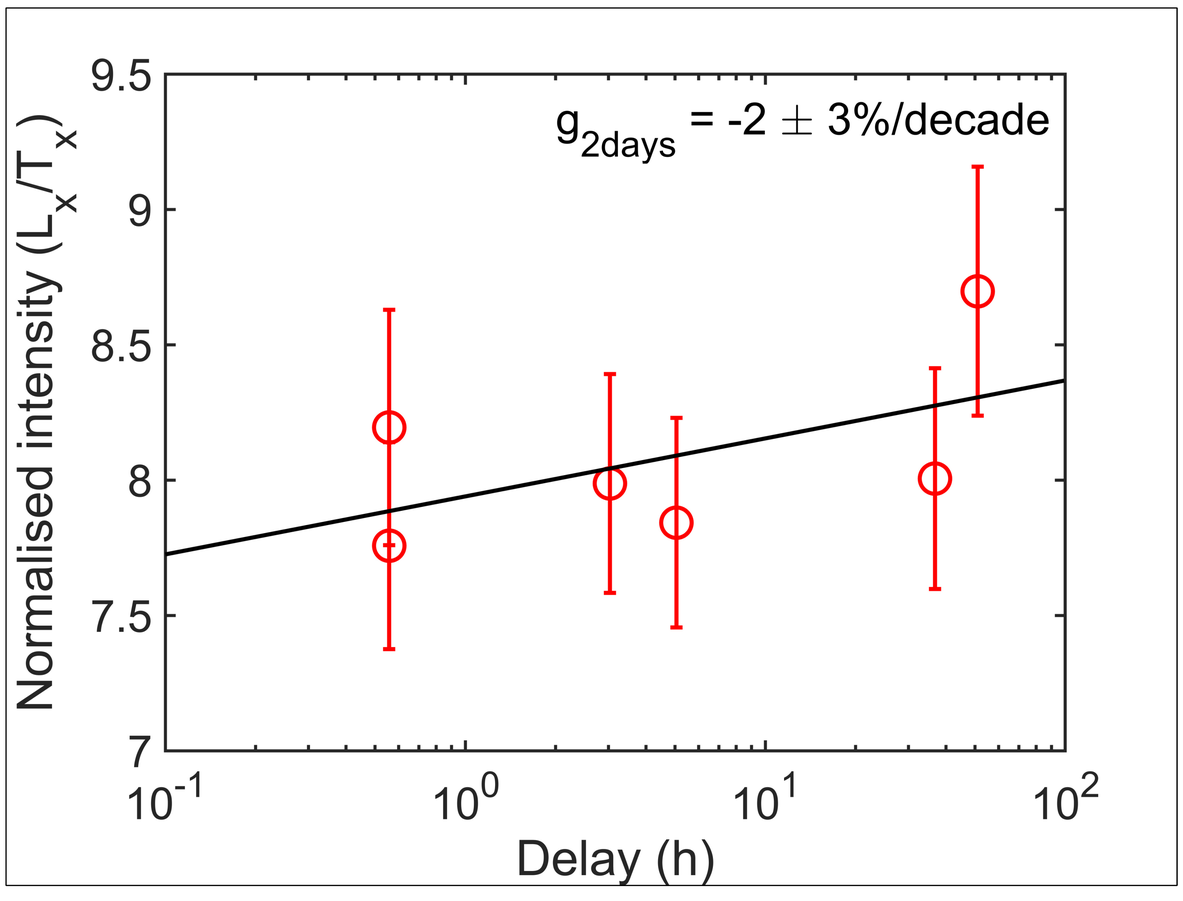
Normalised intensity (L_x/T_x)
Delay (h)
g_{2days} = -2 ± 3%/decade
7
7.5
8
8.5
9
9.5
10^{-1}
10^{0}
10^{1}
10^{2}

d

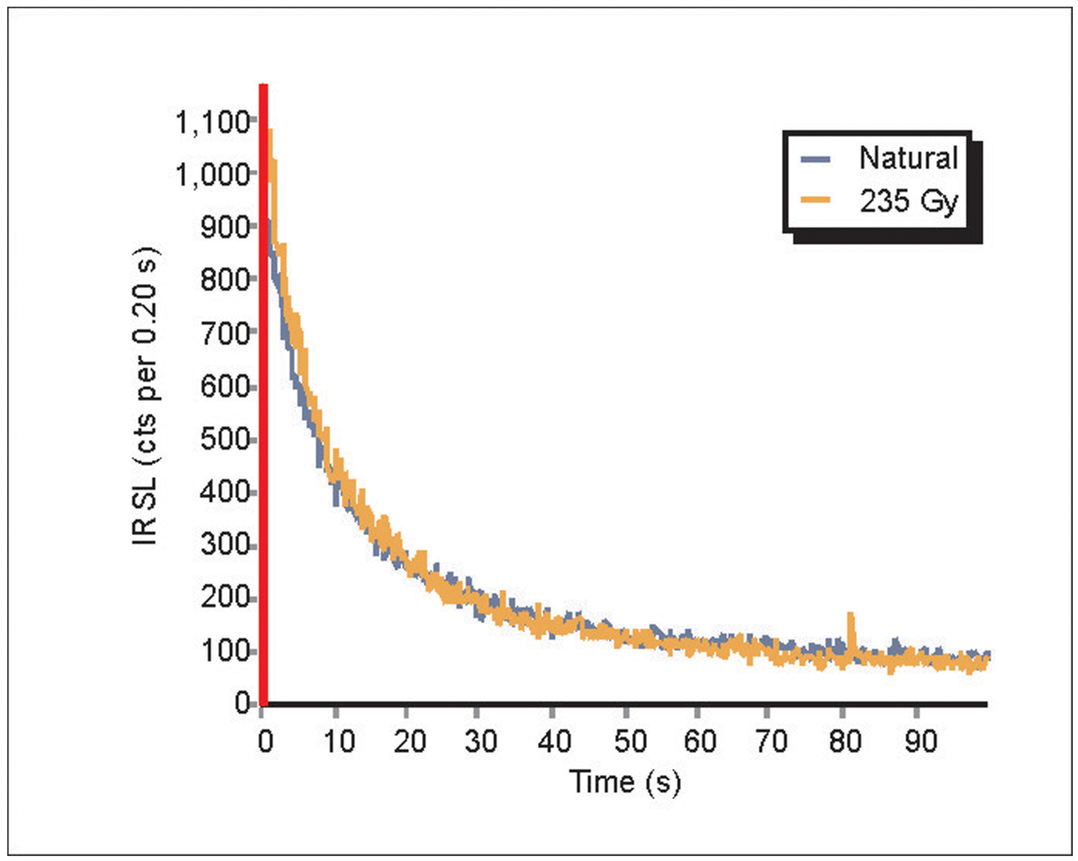
IR SL (cts per 0.20 s)
1,100
1,000
900
800
700
600
500
400
300
200
100
0
0
10
20
30
40
50
60
70
80
90
Time (s)
Natural
235 Gy

a

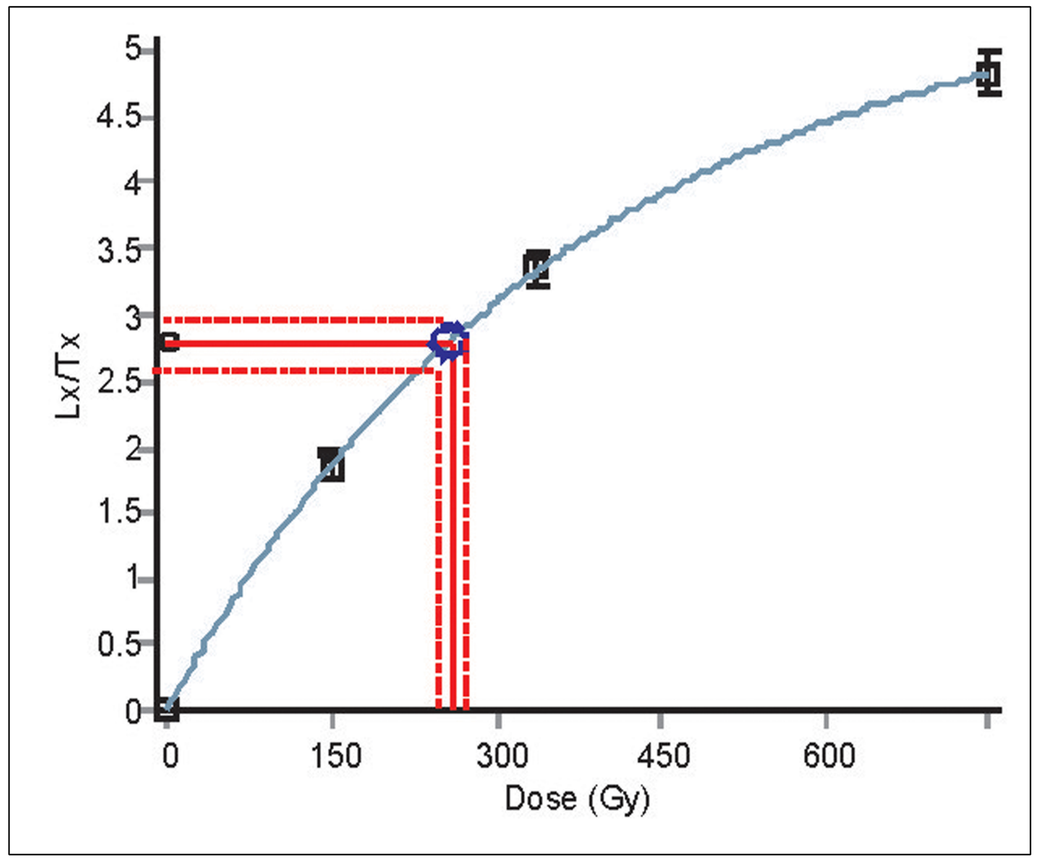
Lx/Tx
5
4.5
4
3.5
3
2.5
2
1.5
1
0.5
0
0
150
300
450
600
Dose (Gy)

b

RTP-18-2

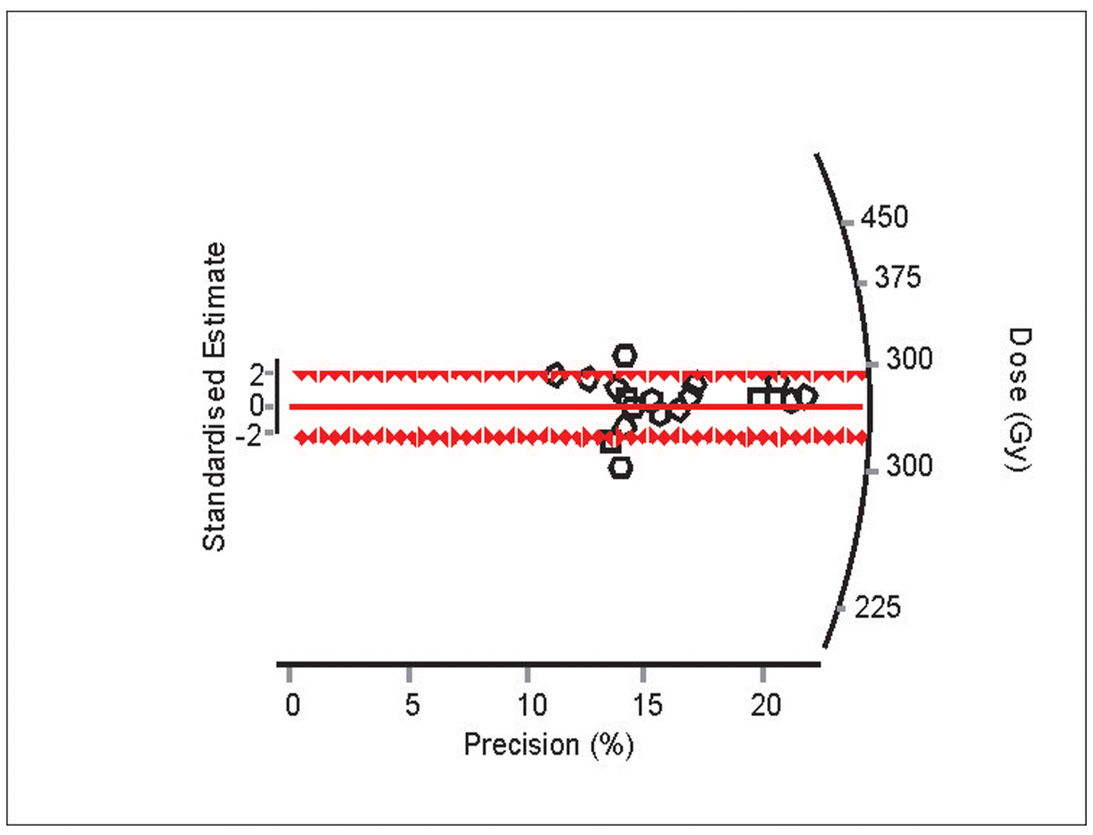
Standardised Estimate
2
0
-2
450
375
300
300
225
Dose (Gy)
0
5
10
15
20
Precision (%)

c

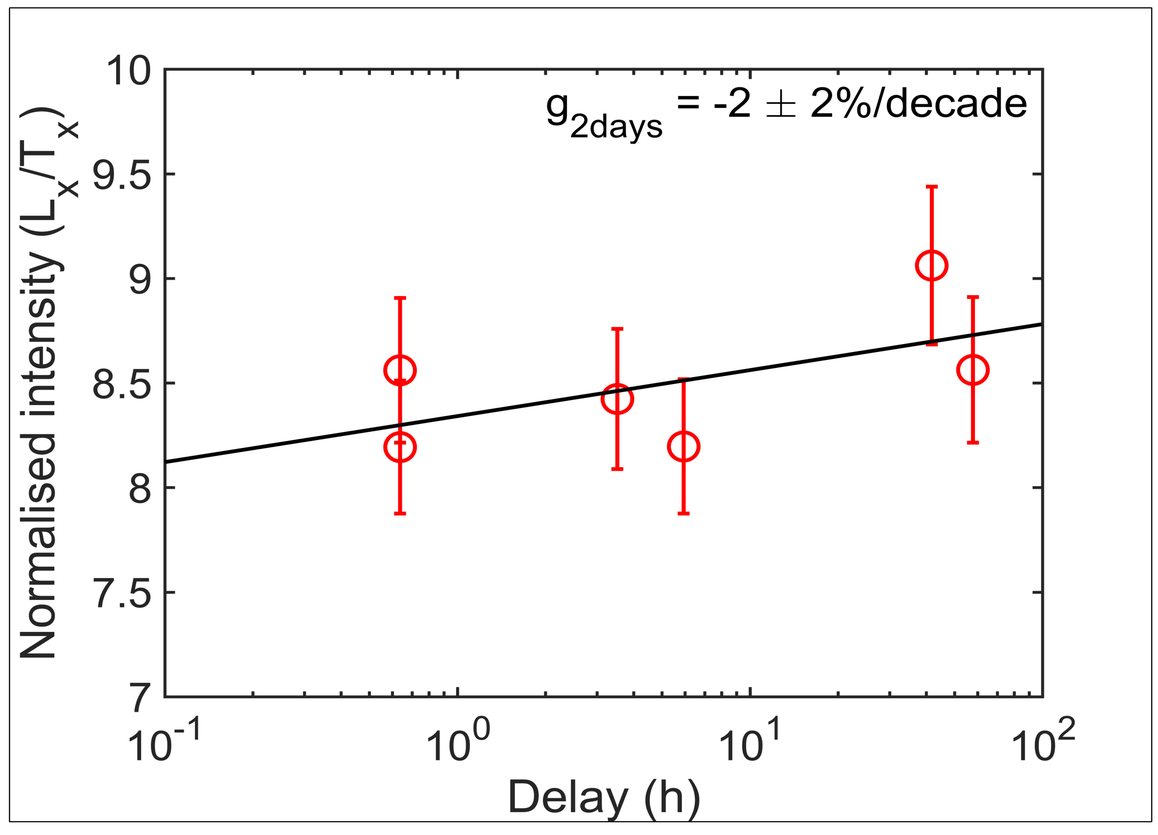
Normalised intensity (Lx/Tx)
g2days = -2 ± 2%/decade
10
9.5
9
8.5
8
7.5
7
10-1
100
101
102
Delay (h)

d

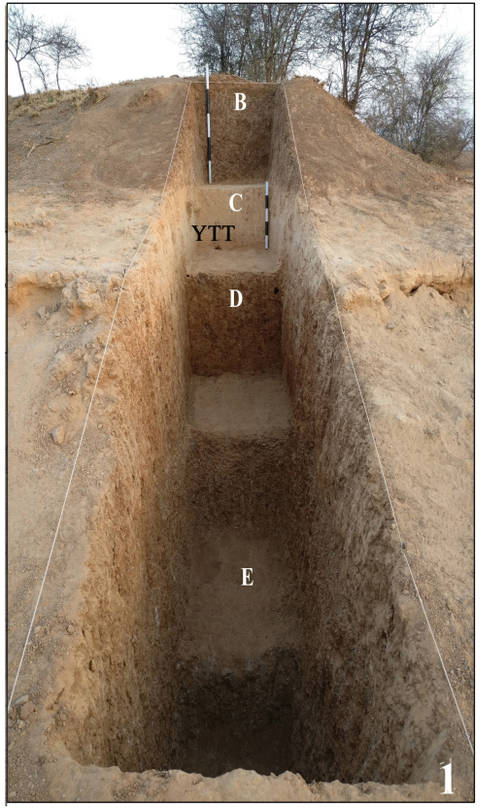

OSL Sample
Sediment Sample
Silt
Sand
Clay
Organic Matter
Carbonate

Depth in cm
0 cm
Layer B
64.4 ± 3.9 ka
100
YTT
Layer C
Layer D
76.3 ± 5.5 ka
200
Layer E
Middle Paleolithic Artefacts
300

0 50 100%
0 10 20%
XLF
0 10
XFD%
0 15

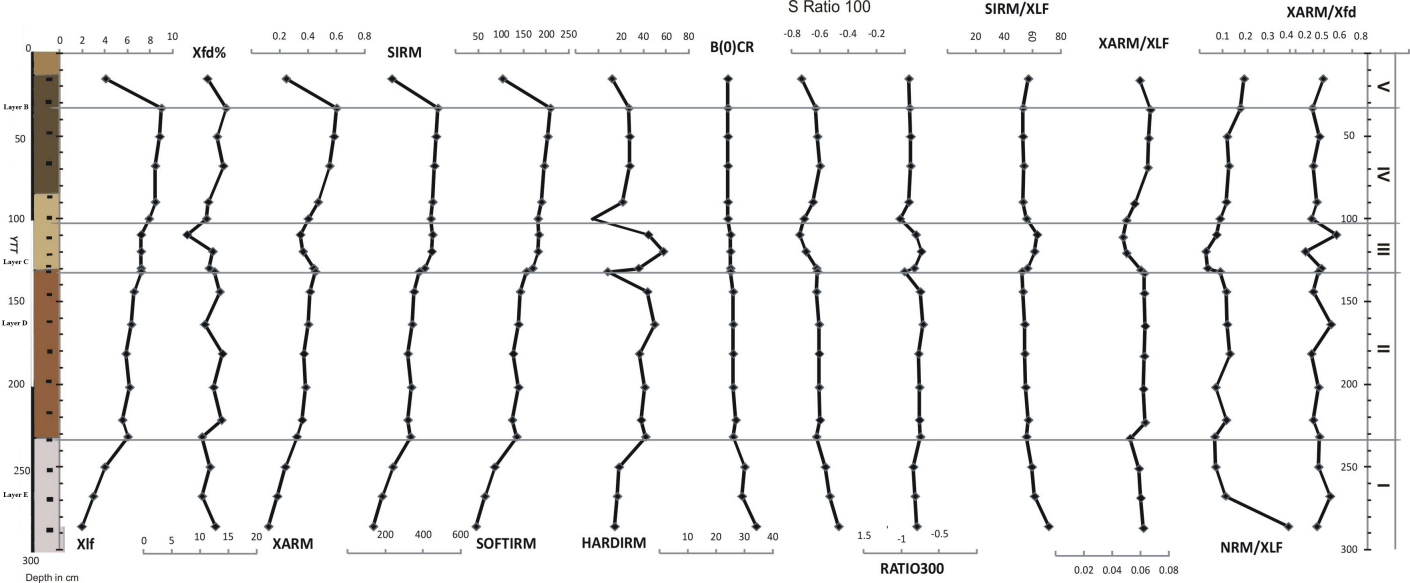
Xfd%
SIRM
B(0)CR
S Ratio 100
SIRM/XLF
XARM/XLF
XARM/Xfd
Xlf
XARM
SOFTIRM
HARDIRM
RATIO300
NRM/XLF
Layer B
Layer C
Layer D
Layer E
V
IV
III
II
I
Depth in cm

a

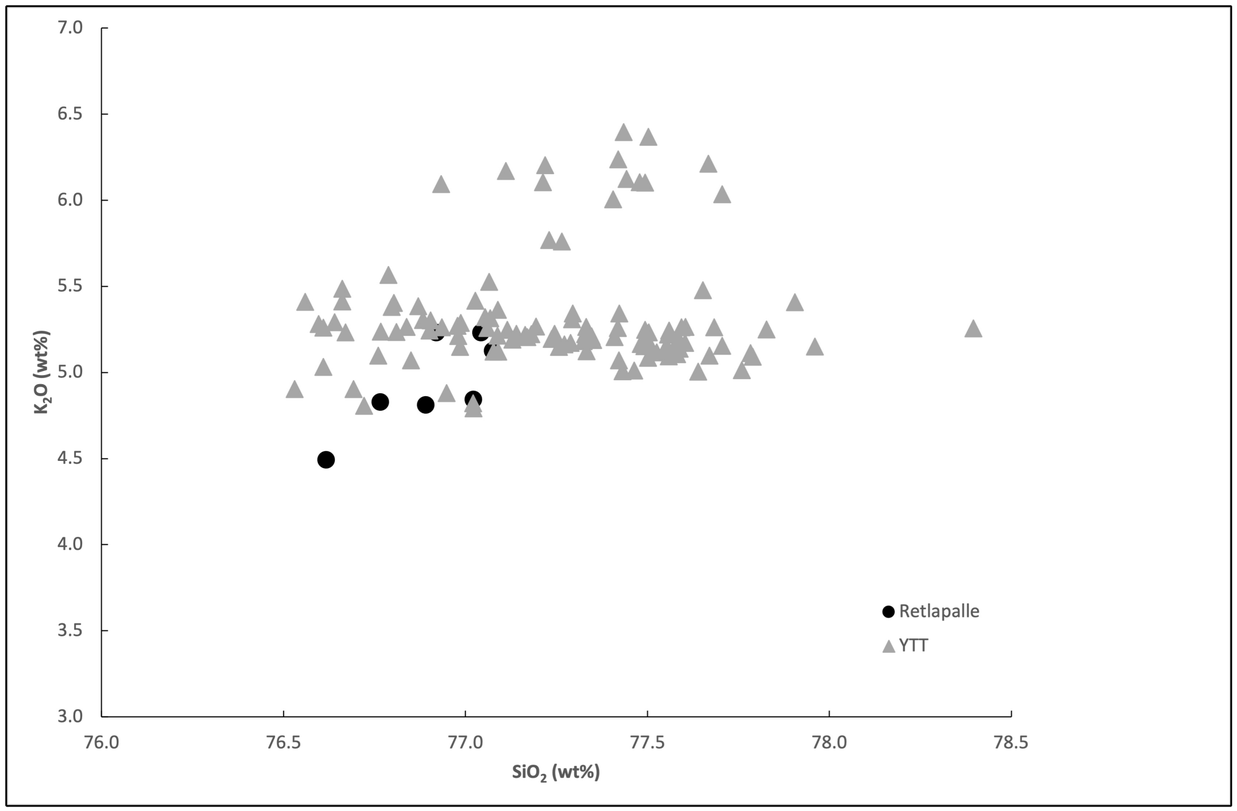
7.0
6.5
6.0
5.5
5.0
4.5
4.0
3.5
3.0
K2O (wt%)
76.0
76.5
77.0
77.5
78.0
78.5
SiO2 (wt%)
Retlapalle
YTT

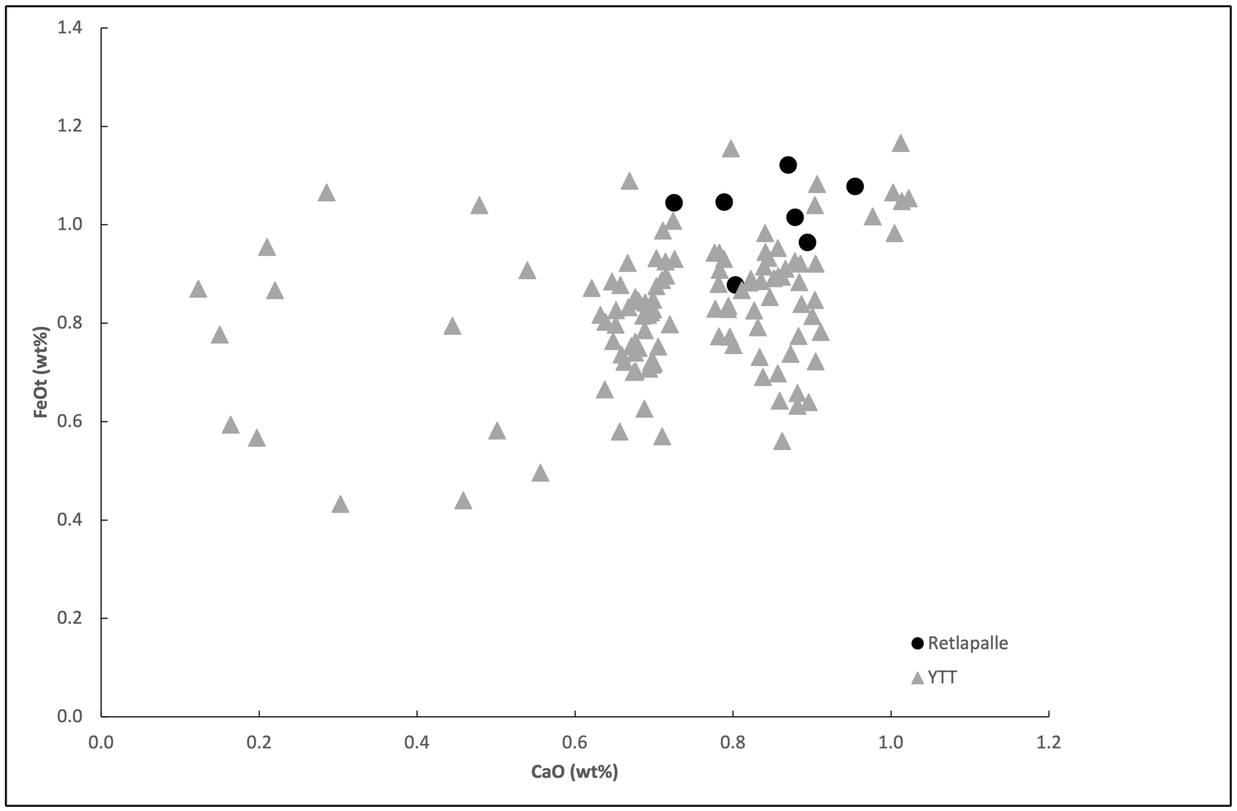
1.4
1.2
1.0
0.8
0.6
0.4
0.2
0.0
FeOt (wt%)
0.0
0.2
0.4
0.6
0.8
1.0
1.2
CaO (wt%)
Retlapalle
YTT

b

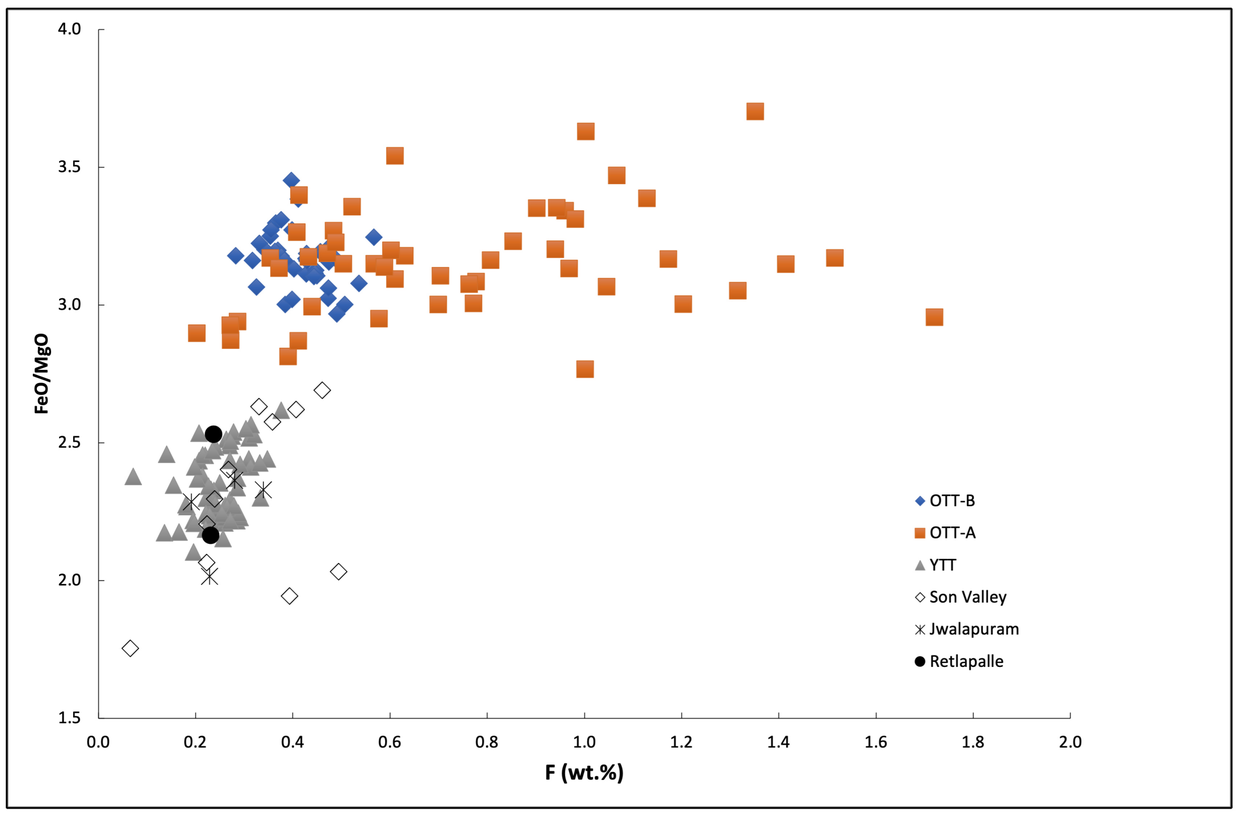
4.0
3.5
3.0
2.5
2.0
1.5
FeO/MgO
0.0
0.2
0.4
0.6
0.8
1.0
1.2
1.4
1.6
1.8
2.0
F (wt.%)
OTT-B
OTT-A
YTT
Son Valley
Jwalapuram
Retlapalle

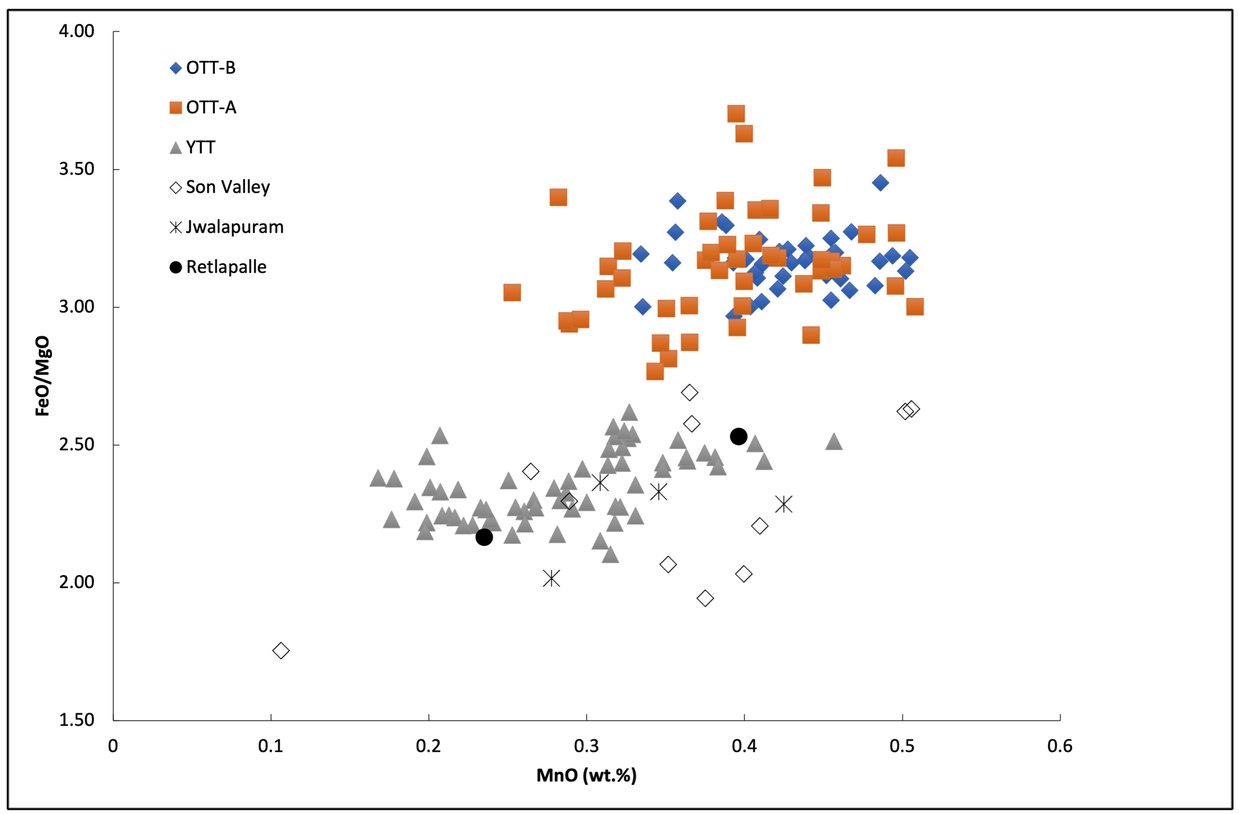
4.00
3.50
3.00
2.50
2.00
1.50
FeO/MgO
0
0.1
0.2
0.3
0.4
0.5
0.6
MnO (wt.%)
OTT-B
OTT-A
YTT
Son Valley
Jwalapuram
Retlapalle

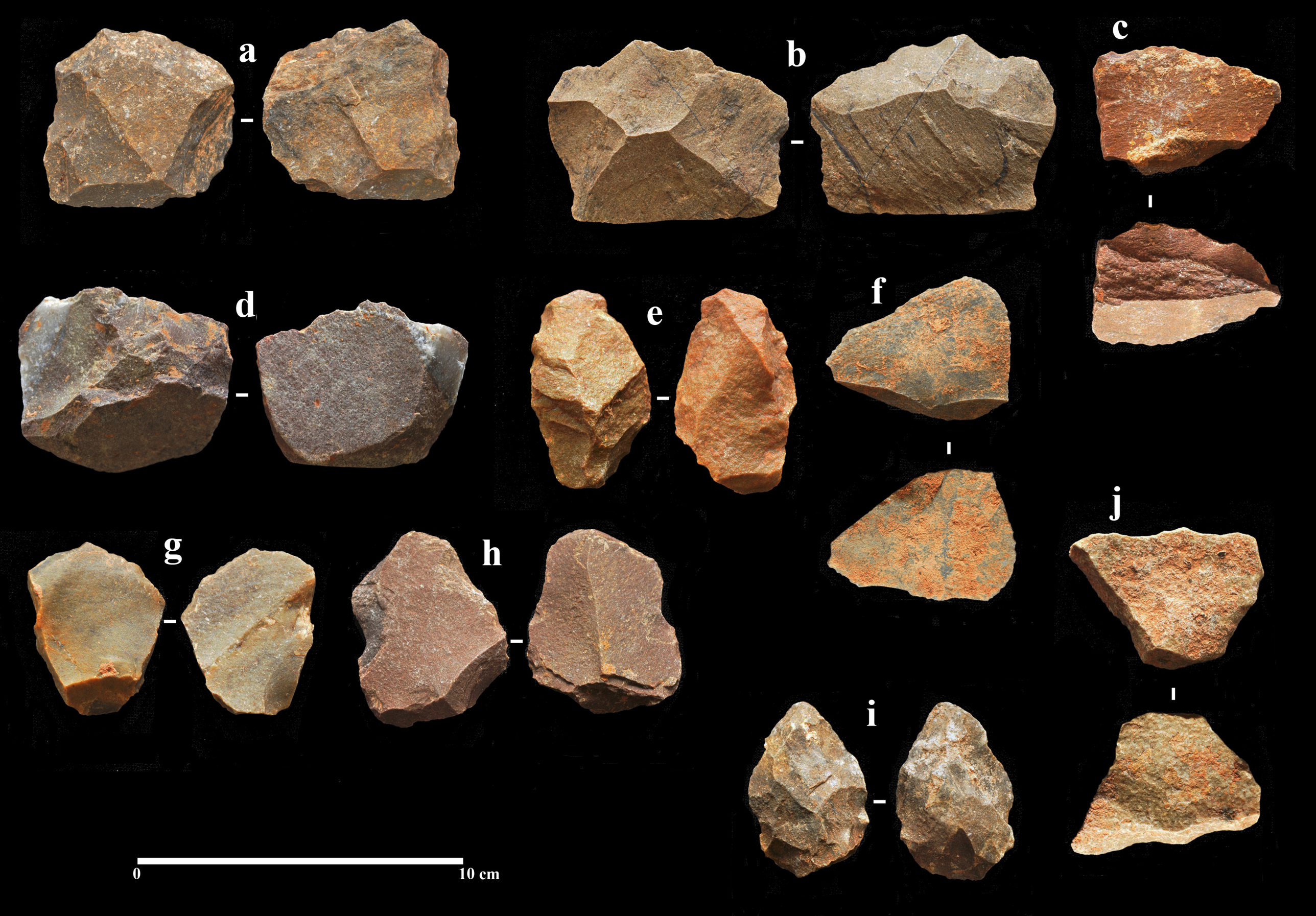
a
b
c
d
e
f
g
h
i
j
0
10 cm